

# Synthesis and Characterization of Gallium(III) 2-Hydroxy-5,10,15,20-tetraphenylporphyrin. A Novel Example of a Cyclic Gallium(III) Porphyrin Trimer<sup>†</sup>

Jacek Wojaczyński and Lechosław Latos-Grażyński\*

Institute of Chemistry, University of Wrocław, 14 F. Joliot-Curie St., Wrocław 50 383, Poland

Received July 7, 1994<sup>®</sup>

A trimeric [(2-O-TPP)Ga<sup>III</sup>]<sub>3</sub> complex (2-O-TPP is a trianion of 2-hydroxy-5,10,15,20-tetraphenylporphyrin) was obtained by hydrolysis of the monomeric five-coordinate complex (2-BzO-TPP)Ga<sup>III</sup>Cl (2-BzO-TPP is a dianion of 2-benzoyloxy-5,10,15,20-tetraphenylporphyrin) with sodium hydroxide in ethanol. The <sup>1</sup>H NMR spectra of the trimer and its monomeric precursors: (2-BzO-TPP)Ga<sup>III</sup>Cl, (2-OH-TPP)Ga<sup>III</sup>TFA are presented and analyzed. The spectroscopic evidences indicated that the trimeric gallium(III) complex has a head-to-tail cyclic trimeric structure with the pyrrolic-alkoxide groups forming bridges from one macrocycle to the metal in the adjacent macrocycle PGa–O–PGa–O–PGa–O. The three gallium(III) porphyrin subunits are not equivalent. Their spatial proximity produces a marked variation of the chemical shifts due to a contribution of the ring current effect. The unprecedented positions of the 3-H pyrrole resonances (1.82, 2.18, 2.82 ppm), when compared to (2-BzO-TPP)Ga<sup>III</sup>Cl (8.96 ppm), reflect the coordination of 2-O centers to the adjacent gallium(III) ions. The strong effects were also determined for ortho 20-phenyl resonances ([ (2-O-TPP)Ga<sup>III</sup> ]<sub>3</sub>, 5.21, 5.36, 5.69, 5.78, 5.93, and 6.33 ppm; (2-BzO-TPP)Ga<sup>III</sup>Cl, 7.9–8.4 ppm). A two-dimensional COSY experiment was effective in connecting the protons within the phenyl and pyrrole rings. The complete peak assignments were derived from the NOESY experiment. In particular, closed loops of the NOE connectivities, which involved interporphyrin contacts between all subunits of the trimer, were analyzed and provided unambiguous spectroscopic evidence for the cyclic trimer formation. The trimer was cleaved in the reversible process to the monomeric complexes: (2-OH-TPP)Ga<sup>III</sup>Cl and [(2-O-TPP)Ga<sup>III</sup>(OH)]<sup>−</sup> by addition of HCl or OH<sup>−</sup>, respectively. The formation of the expanded linear intermediate was demonstrated in the course of the acidic cleavage. The differences of pyrrole chemical shifts demonstrated for the gallium(III) monomeric species and the increased lability of the 3-H pyrrole proton resulted from the tautomeric phenol–enol–ketone equilibria typical for the 2-OH-TPPH<sub>2</sub> porphyrin.

## Introduction

Oligomeric porphyrins and metalloporphyrins of various structures are under intensive investigation due to their relevance to the mechanism of photosynthesis and their potential application in molecular electronics.<sup>1–3</sup> The intense studies of oligomeric metalloporphyrins are aimed at generating artificial allosteric systems.<sup>4</sup> Polymetalloporphyrins were investigated as polyelectron redox molecular catalysts in the four-electron reduction of dioxygen<sup>5</sup> or in proton reduction.<sup>6</sup>

Dimeric metalloporphyrins are usually assembled using a diversity of links such as formation of a bridge between two metal ions by bidentate ligands,<sup>7</sup> a covalent bond at the porphyrin ligand peripheries,<sup>4–6,8</sup> and a direct metal–metal bond.<sup>9</sup> The double decker metalloporphyrins P<sub>2</sub>M present a specific case where a metal ion serves as a bridging unit.<sup>10</sup> The complexes of monohydroxy-substituted porphyrins, i.e. 5-(2-

\* Author to whom correspondence should be addressed.

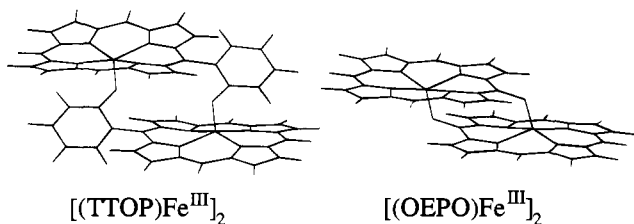
<sup>†</sup> Abbreviations used: P, porphyrin dianion; TPP, 5,10,15,20-tetraphenylporphyrin dianion; OEP, octaethylporphyrin dianion; TTOP, 5-(2-hydroxyphenyl)-10,15,20-tritylporphyrin trianion; OEPO, 5-hydroxyoctaethylporphyrin (oxophlorin) trianion; 2-OH-TPP, dianion of 2-hydroxy-5,10,15,20-tetraphenylporphyrin; 2-O-TPP, trianion of 2-hydroxy-5,10,15,20-tetraphenylporphyrin; 2-OH-TPP-*d*<sub>20</sub>, dianion of 2-hydroxy-5,10,15,20-tetraphenylporphyrin deuterated at *meso*-phenyl positions; 2-OH-TPP-*d*<sub>6</sub>, dianion of 2-hydroxy-5,10,15,20-tetraphenylporphyrin deuterated at 6,7-, 12,13,17,18 pyrrole positions; 2-O-TPP-*d*<sub>20</sub> and 2-O-TPP-*d*<sub>6</sub>, corresponding deuterated trianions; 2-BzO-TPP, dianion of 2-benzoyloxy-5,10,15,20-tetraphenylporphyrin; 2-BzO-TPP-*d*<sub>7</sub>, dianion of 2-benzoyloxy-5,10,15,20-tetraphenylporphyrin deuterated at pyrrole positions.

<sup>®</sup> Abstract published in *Advance ACS Abstracts*, February 1, 1995.

- (1) (a) Wasielewski, R. *Chem. Rev.* **1992**, *48*, 8781. (b) Gust, D.; Moore, T. A. *Topics in Current Chemistry*; Springer-Verlag: Berlin 1991; Vol. 159, pp 103–156.
- (2) (a) Crossley, M. J.; Burn, P. L. *J. Chem. Soc., Chem. Commun.* **1987**, 39. (b) Crossley, M. J.; Burn, P. L. *J. Chem. Soc., Chem. Commun.* **1991**, 1569.
- (3) (a) Cosmo, R.; Kautz, C.; Meerholz, K.; Heinze, J.; Müllen, K. *Angew. Chem., Int. Ed. Engl.* **1989**, *28*, 604. (b) Lambrate, A.; Momeanteau, M.; Maillard, P.; Seta, P. *J. Mol. Electron.* **1990**, *6*, 145. (c) Ono, N.; Tomita, H.; Maruyama, K. *J. Chem. Soc., Perkin Trans. 1* **1992**, 2453.
- (4) Tabushi, I. *Pure Appl. Chem.* **1988**, *60*, 581.

- (5) (a) Ni, C.-L.; Abdalmuhi, I.; Chang, C. K.; Anson, F. C. *J. Phys. Chem.* **1987**, *91*, 1158. (b) Collman, J. P.; Hutchison, J. E.; Lopez, M. A.; Tabard, A.; Guillard, R.; Seok, W. K.; Ibers, J. A.; L'Her, M. *J. Am. Chem. Soc.* **1992**, *114*, 9689.
- (6) Collman, J. P.; Ha, Y.; Wagenknecht, P. S.; Lopez, M.-A.; Guillard, R. *J. Am. Chem. Soc.* **1993**, *115*, 9080.
- (7) (a) Fleischer, E. B.; Palmer, J. M.; Sristava, T. S.; Chatterjee, A. *J. Am. Chem. Soc.* **1971**, *93*, 3162. (b) Summerville, D. A.; Cohen, I. A. *J. Am. Chem. Soc.* **1976**, *98*, 1747. (c) Mansuy, D.; Lecomte, J.-P.; Chottard, J.-C.; Bartoli, J.-F. *Inorg. Chem.* **1981**, *20*, 3119. (d) Phillippi, M. A.; Baenzinger, N.; Goff, H. M. *Inorg. Chem.* **1981**, *20*, 3904. (e) Chin, D.-H.; La Mar, G. N.; Balch, A. L. *J. Am. Chem. Soc.* **1980**, *102*, 4344. (f) Landrum, J. T.; Grimmett, D.; Haller, K. J.; Scheidt, W. R.; Reed, C. A. *J. Am. Chem. Soc.* **1981**, *103*, 2640. (g) Fuhrhop, J.-H.; Baccouche, M.; Bünzel, M. *Angew. Chem., Int. Ed. Engl.* **1980**, *19*, 322. (h) Kessel, S. L.; Hendrickson, D. N. *Inorg. Chem.* **1980**, *19*, 1883. (i) Boersma, A. D.; Goff, H. M. *Inorg. Chim. Acta* **1984**, *89*, L49. (j) Shin, K.; Yu, B.-S.; Goff, H. M. *Inorg. Chem.* **1990**, *29*, 889.
- (8) (a) Dolphin, D.; Hiom, J.; Paine, J. B., III *Heterocycles* **1981**, *16*, 417. (b) Dixon, D. B.; Kumar, V. *New J. Chem.* **1992**, *16*, 555 and references cited therein.
- (9) Collman, J. P.; Arnold, H. J. *Acc. Chem. Res.* **1993**, *26*, 586 and references cited therein.
- (10) (a) Buchler, J. W.; de Cian, A.; Fischer, J.; Kihn-Botulinski, M.; Paulus, R.; Weiss, R. *J. Am. Chem. Soc.* **1986**, *108*, 3652. (b) Girolami, G. S.; Milam, S. N.; Suslick, K. S. *J. Am. Chem. Soc.* **1988**, *110*, 2011.

hydroxyphenyl)-10,15,20-tritylporphyrin and 5-hydroxyoctaethylporphyrin (oxophlorin) with trivalent metal ions, dimerize to give the doubly oxo bridged head-to-tail structural arrangements of general formula  $[(\text{TTOP})\text{M}^{\text{III}}]_2$  or  $[(\text{OEPO})\text{M}^{\text{III}}]_2$ .<sup>11–13</sup>



Trimeric or highly oligomeric porphyrins and metalloporphyrins are less common.<sup>14</sup> The flexible covalent bridging allowed the construction of linearly arranged tris(porphyrins).<sup>14b–e</sup> Fully conjugated, coplanar tetrakis(porphyrin), linked by fused aromatic rings, was synthesized in an attempt to generate a molecular wire.<sup>2</sup> Routes to design and synthesize trimeric cyclic porphyrins and metalloporphyrins, connected by butadiyne or alkyne–platinum–alkyne units, were also established.<sup>15</sup> Other cases of metalloporphyrins incorporated into the oligomer backbone are exemplified by  $[\text{PFe}^{\text{III}}(\text{imidazolate})]_n$ <sup>16</sup> and a series of the triple decker metalloporphyrins  $\text{P}_3\text{M}_2$ .<sup>17</sup>

Recently we have synthesized and characterized the unprecedented cyclic iron(III) porphyrin trimer  $[(2\text{-O-TPP})\text{Fe}^{\text{III}}]_3$ .<sup>18</sup> This compound was the product of oligomerization of iron(III) 2-hydroxy-5,10,15,20-tetraphenylporphyrin. The ligand is the tetraphenylporphyrin derivative which is hydroxylated at a  $\beta$ -pyrrolic position. An equilibrium between enol, keto, and aromatic hydroxyl tautomers was observed for 2-OH-TPPH<sub>2</sub> and its complexes.<sup>19</sup> The 2-hydroxy-5,10,15,20-tetraphenylporphyrin molecule presents properties of hybrid bifunctional ligands as it contains two centers of coordination. This structural feature is critical for the trimerization.

Here we sought to extend our investigations from the paramagnetic iron(III) complexes to the diamagnetic gallium(III) ones in order to take full advantage of the structural

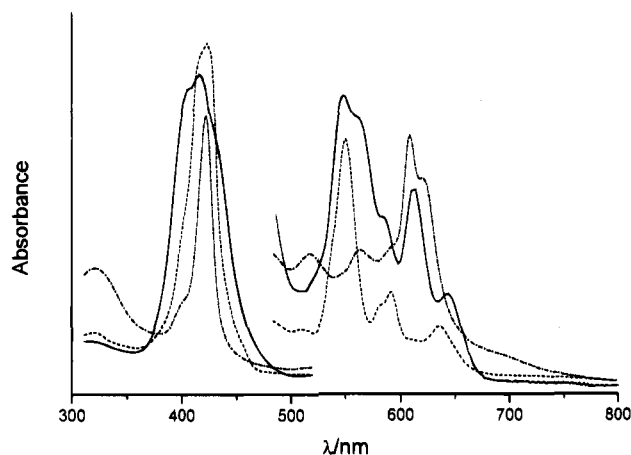


**Figure 1.** UV–vis spectra of  $[(2\text{-O-TPP})\text{Ga}^{\text{III}}]_3$  (solid line),  $(2\text{-OH-TPP})\text{Ga}^{\text{III}}\text{Cl}$  (dashed line), and  $[(2\text{-O-TPP})\text{Ga}^{\text{III}}(\text{OH})]^-$  (dot–dashed line) in dichloromethane.

characterization by way of two-dimensional <sup>1</sup>H NMR experiments (COSY, NOESY, ROESY), supported by molecular mechanics calculations. In this paper we present our studies of the  $(2\text{-OH-TPP})\text{Ga}^{\text{III}}\text{Cl}$  oligomerization process, which led to the identification of a novel example of a cyclic diamagnetic metalloporphyrin trimer.

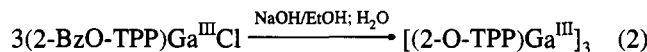
## Results and Discussion

**Synthesis and Characterization of  $[(2\text{-O-TPP})\text{Ga}^{\text{III}}]_3$ .** In order to produce gallium(III) 2-hydroxy-tetraphenylporphyrin complexes the  $\beta$ -benzoyloxy derivative 2-benzoyloxy-TPPH<sub>2</sub> was prepared by a route that involves benzylation of tetraphenylporphyrin,<sup>20</sup> followed by the chromatographic separation of the monosubstituted product.



(BzO<sub>2</sub>) = benzoyl peroxide

Gallium(III) is readily inserted into 2-benzoyloxy–TPPH<sub>2</sub> to give  $(2\text{-BzO-TPP})\text{Ga}^{\text{III}}\text{Cl}$ . Basic hydrolysis of this complex resulted in formation of a novel cyclic trimeric molecule:



Addition of acids in excess (HX: HCl, HBr, TFA) to  $[(2\text{-O-TPP})\text{Ga}^{\text{III}}]_3$  has cleaved the trimer to a monomeric species  $(2\text{-OH-TPP})\text{Ga}^{\text{III}}\text{X}$ . The process can be reversed by addition of a proton scavenger such as 2,4,6-collidine. This fact has been proven by means of the UV–vis spectroscopy. The electronic spectrum of  $[(2\text{-O-TPP})\text{Ga}^{\text{III}}]_3$  is presented in Figure 1 together with the spectra of  $(2\text{-OH-TPP})\text{Ga}^{\text{III}}\text{Cl}$  and  $[(2\text{-O-TPP})\text{Ga}^{\text{III}}(\text{OH})]^-$  (vide infra). The electronic spectra of  $(2\text{-OH-TPP})\text{Ga}^{\text{III}}\text{Cl}$  and  $(2\text{-BzO-TPP})\text{Ga}^{\text{III}}\text{Cl}$  (not shown) are typical for five-coordinate gallium(III) tetraphenylporphyrins while the electronic spectrum of  $[(2\text{-O-TPP})\text{Ga}^{\text{III}}]_3$  differs considerably from its precursors and from any five-coordinate gallium(III) tetraphenylporphyrin species.<sup>21,22</sup> The Soret band shows a blue shift, and all bands are broadened as compared to those observed for  $(2\text{-OH-TPP})\text{Ga}^{\text{III}}\text{Cl}$ . The differences may be induced by the 2-oxygen coordination to the adjacent gallium(III) ion. The

(20) Callot, H. *Bull. Soc. Chim. Fr.* **1974**, 1492.

(21) Kadish, K. M.; Comillon, J.-L.; Coutsolelos, A.; Guillard, R. *Inorg. Chem.* **1987**, *26*, 4167.

(22) Balch, A. L.; Latos-Grażyński, L.; Noll, B. C.; Phillips, S. L. *Inorg. Chem.* **1993**, *32*, 1124.

- (11) Masuoka, N.; Itano, H. A. *Biochemistry* **1987**, *26*, 3672.  
 (12) (a) Balch, A. L.; Latos-Grażyński, L.; Noll, B. C.; Olmstead, M. M.; Zovinka, E. P. *Inorg. Chem.* **1992**, *31*, 2248. (b) Balch, A. L.; Noll, B. C.; Reid, S. M.; Zovinka, E. P. *Inorg. Chem.* **1993**, *32*, 2610. (c) Balch, A. L.; Noll, B. C.; Olmstead, M. M.; Reid, S. M. *J. Chem. Soc., Chem. Commun.* **1993**, *32*, 1088.  
 (13) (a) Goff, H. M.; Shimomura, E. T.; Lee, Y. J.; Scheidt, W. R. *Inorg. Chem.* **1984**, *23*, 315. (b) Godziela, G. M.; Tilotta, D.; Goff, H. M. *Inorg. Chem.* **1986**, *25*, 2142.  
 (14) (a) Kadish, K. M.; Liu, Y. H.; Anderson, J. E.; Charpin, P.; Chevrier, G.; Lance, M.; Nierlich, M.; Vigner, D.; Dormond, A.; Belkalem, B.; Guillard, R. *J. Am. Chem. Soc.* **1988**, *110*, 6455. (b) Ichimura, K.; Takeuchi, S. *Heterocycles* **1978**, *1*, 96. (c) Anton, J. A.; Kwong, J.; Loach, P. A. *J. Heterocycl. Chem.* **1976**, *13*, 717. (d) Lin, V. S.-Y.; DiMaggio, S. G.; Therien, M. *J. Inorg. Biochem.* **1993**, *51*, 163. (e) Sessler, J. L.; Capuano, V. L. *Angew. Chem., Int. Ed. Engl.* **1990**, *29*, 1134.  
 (15) (a) Anderson, H. L.; Sanders, J. K. M. *Angew. Chem., Int. Ed. Engl.* **1990**, *29*, 1400. (b) Mackay, L. G.; Anderson, H. L.; Sanders, J. K. M. *J. Chem. Soc., Chem. Commun.* **1992**, *44*. (c) Anderson, H. L.; Sanders, J. K. M. *J. Chem. Soc., Chem. Commun.* **1992**, *146*. (d) Anderson, S.; Anderson, H. L.; Sanders, J. K. M. *Angew. Chem., Int. Ed. Engl.* **1992**, *31*, 907.  
 (16) Landrum, J. T.; Reed, C. A.; Hatano, K.; Scheidt, R. W. *Inorg. Chem.* **1978**, *100*, 3232.  
 (17) Buchler, J. W.; de Cian, A.; Fischer, J.; Kihn-Botulinski, M.; Weiss, R. *Inorg. Chem.* **1988**, *27*, 339.  
 (18) Wojaczyński, J.; Latos-Grażyński, L. *Inorg. Chem.* **1995**, *34*, 1044.  
 (19) (a) Crossley, M. J.; King, L. G.; Pyke, S. M. *Tetrahedron* **1987**, *43*, 4569. (b) Crossley, M. J.; Harding, M. M.; Sternhell, S. *J. Am. Chem. Soc.* **1986**, *108*, 3608. (c) Crossley, M. J.; Field, L. D.; Harding, M. M.; Sternhell, S. *J. Am. Chem. Soc.* **1987**, *109*, 2335. (d) Crossley, M. J.; Harding, M. M.; Sternhell, S. *J. Org. Chem.* **1988**, *53*, 1132. (e) Crossley, M. J.; Burn, P. L.; Langford, S. J.; Pyke, S. M.; Stark, A. G. *J. Chem. Soc., Chem. Commun.* **1991**, 1567.

**Table 1.**  $^1\text{H}$  NMR Chemical Shifts [ppm] for  $[(2\text{-O-TPP})\text{Ga}^{\text{III}}]_3^a$ 

proton	unit			
	S	R <sub>1</sub>	R <sub>2</sub>	
pyrrole <sup>b</sup>	3-H	2.18	1.82	2.82
	7-H	8.55	8.49	8.81
	8-H	8.92	8.68	9.00
	12-H	8.80	8.79	8.63
	13-H	8.88	8.72	8.72
	17-H	8.20	8.54	8.23
	18-H	7.48	7.88	7.36
	<i>meso</i> -phenyl	5-Ph <i>o</i> <sub>1</sub>	7.28	6.87
<i>m</i> <sub>1</sub>		7.45	7.40	7.57
<i>p</i>		7.67	7.74	7.97
<i>m</i> <sub>2</sub>		7.67	7.9 <sup>c</sup>	8.31
<i>o</i> <sub>2</sub>		8.08	8.47	9.07
10-Ph <i>o</i> <sub>1</sub>		7.51	7.96	8.05
<i>m</i> <sub>1</sub>		7.6 <sup>c</sup>	7.73	7.72
<i>p</i>		7.80	7.6–7.9 <sup>c</sup>	7.68
<i>m</i> <sub>2</sub>		8.05	7.75–7.8 <sup>c</sup>	7.75–7.8 <sup>c</sup>
<i>o</i> <sub>2</sub>		8.89	8.17	8.16
15-Ph <i>o</i> <sub>1</sub>		7.79	7.64	7.69
<i>m</i> <sub>1</sub>		7.6 <sup>c</sup>	7.7 <sup>c</sup>	7.6 <sup>c</sup>
<i>p</i>		7.63	7.75	7.77
<i>m</i> <sub>2</sub>		7.72	7.91	7.85
<i>o</i> <sub>2</sub>		8.22	8.58	8.30
20-Ph <i>o</i> <sub>1</sub>		5.36	5.93	5.21
<i>m</i> <sub>1</sub>		6.49	6.51	6.45
<i>p</i>		7.00	7.13	6.80
<i>m</i> <sub>2</sub>		6.89	6.64	6.37
<i>o</i> <sub>2</sub>		5.78	6.33	5.69

<sup>a</sup> The spectrum obtained in chloroform-*d* at 243.2 K. <sup>b</sup> Pyrrole-3-H = singlets; other pyrrole resonances present AB patterns ( $^3J_{\text{AB}} = 5$  Hz). <sup>c</sup> The strong overlapping of the phenyl resonances in the 7.6–7.9 ppm region precludes the precise shift determination.

porphyrin–porphyrin  $\pi$  interaction, caused by the proximity of the porphyrin rings in the close-packed trimeric structure, seems to play an essential role as well.<sup>23</sup> The trimeric structure also causes noticeable changes of the fluorescence spectra as revealed by comparison of the  $[(2\text{-O-TPP})\text{Ga}^{\text{III}}]_3$  and  $(2\text{-OH-TPP})\text{Ga}^{\text{III}}\text{-Cl}$  data in Figure 2.

The liquid matrix secondary ion mass spectrum of  $[(2\text{-O-TPP})\text{Ga}^{\text{III}}]_3$  shows peaks due to the parental species  $[(2\text{-O-TPP})\text{Ga}^{\text{III}}]_3$  at  $(m + 1)/z = 2092$  (2.5%) and its stepwise deoligomerization products:  $[(2\text{-O-TPP})\text{Ga}^{\text{III}}]_2$  at  $(m + 1)/z = 1395$  (5%), and  $[(2\text{-O-TPP})\text{Ga}^{\text{III}}]$  at  $(m + 1)/z = 698$  (100%). We have run the control experiments where the trimer has been replaced by monomeric  $(2\text{-OH-TPP})\text{Ga}^{\text{III}}\text{-Cl}$  or  $(2\text{-OH-TPP})\text{Ga}^{\text{III}}\text{-TFA}$  complexes. Apart of the major monomeric forms  $[(2\text{-OH-TPP})\text{Ga}^{\text{III}}]^+$  (100%) and  $(2\text{-OH-TPP})\text{Ga}^{\text{III}}\text{X}$  (X = Cl, TFA, and OH, up to 15%) we have detected small amounts of the dimeric product, probably due to a recombination process in the gas phase ( $[(2\text{-O-TPP})\text{Ga}^{\text{III}}]_2$  (2%)). However, under the conditions of our experiment, the trimeric species has not been formed from either  $(2\text{-OH-TPP})\text{Ga}^{\text{III}}\text{-Cl}$  or  $(2\text{-OH-TPP})\text{Ga}^{\text{III}}\text{-TFA}$ . The presence of  $[(2\text{-O-TPP})\text{Ga}^{\text{III}}]_3$  in the sample seems to be a prerequisite for the observation of the trimeric  $(m + 1)/z = 2092$  peak. Solely on the basis of the mass spectrum, we could not rule out oligomeric structures even higher than the trimeric one since larger ions might not survive in the gas phase.

**$^1\text{H}$  NMR Spectroscopic Studies of  $[(2\text{-O-TPP})\text{Ga}^{\text{III}}]_3$ .** The  $^1\text{H}$  NMR spectrum of  $[(2\text{-O-TPP})\text{Ga}^{\text{III}}]_3$  is shown in Figure 3. The resonance assignments, which are given above selected groups of peaks and are gathered in Table 1, have been made

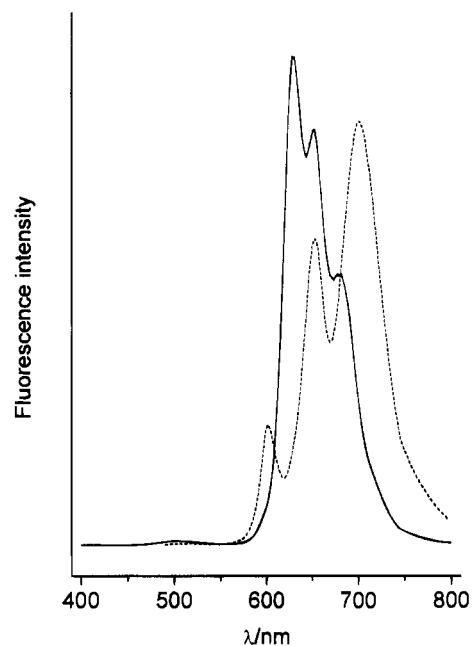


**Figure 2.** Fluorescence spectra of  $[(2\text{-O-TPP})\text{Ga}^{\text{III}}]_3$  (solid line) and  $(2\text{-OH-TPP})\text{Ga}^{\text{III}}\text{-Cl}$  (dashed line) in dichloromethane at 293 K. The excitation wavelengths have been chosen at 350 and 440 nm, respectively, to produce the most intense fluorescence.

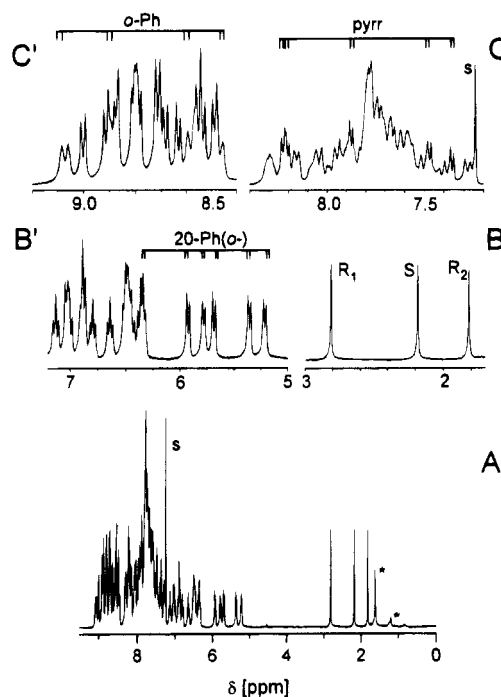


**Figure 3.** 300 MHz  $^1\text{H}$  NMR spectrum of  $[(2\text{-O-TPP})\text{Ga}^{\text{III}}]_3$  in chloroform-*d* at 243 K. Trace A is the entire spectrum while traces B, B' and C, C' demonstrate the expansions of the crowded spectral regions. To clarify the presentation, the resonances in nontypical positions for metalloporphyrins are labeled in each trace as separate sets. Trace B shows 3-H pyrrole resonances located in the 1.8–3.0 ppm region with the individual resonance assignments to a specific porphyrin unit. The upfield shifted phenyl resonances are shown in Trace B' with ortho resonances of 20-Ph marked (20-Ph(*o*-)). In trace C (7.2–8.4 ppm), pyrrole resonances have been labeled as pyr (remaining resonances are due to *meso* phenyl protons). Trace C' demonstrates details of the 8.4–9.2 ppm region. The ortho resonances of phenyl rings have been marked as *o*-Ph (the remaining resonances are due to pyrrole protons). Key: S, solvent; \*, solvent impurities.

on the basis of relative intensities, site specific deuteration and detailed two-dimensional  $^1\text{H}$  NMR studies (COSY, NOESY, ROESY). The proton numbering used in the description of

(23) (a) Osuka, A.; Marruyama, K. *J. Chem. Soc.* **1988**, 110, 4454. (b) Chang, C. K. *Adv. Chem. Ser.* **1979**, 173, 162. (c) Hunter, C. A.; Sanders, J. K. M. *J. Am. Chem. Soc.* **1990**, 112, 5525.

**Table 2.**  $^1\text{H}$  NMR Chemical Shifts [ppm] of Monomeric Gallium(III) Porphyrins<sup>a</sup>

proton		compound		
		(2-OH-TPP)Ga <sup>III</sup> Cl	[(2-O-TPP)Ga <sup>III</sup> (OH)] <sup>-</sup>	(2-BzO-TPP)Ga <sup>III</sup> Cl
pyrrole <sup>b</sup>	3-H	8.24	<i>c</i>	8.96
	7,8-H	9.01, 9.06	8.71, 8.82	9.04, 9.07
	12,13-H	9.04, 9.04	8.77, 8.82	9.05, 9.05
	17,18-H	8.80, 9.03	8.46, 8.72	8.79, 8.98
<i>meso</i> -phenyl	<i>o</i> -	8.0–8.35	7.9–8.1	7.9–8.4
	<i>m</i> -, <i>p</i> -	7.65–7.95	7.5–7.7	7.2–7.8 <sup>d</sup>
OH		6.12		

<sup>a</sup> All spectra measured in chloroform-*d* at 293 K. <sup>b</sup> 7,8-H; 12,13-H; 17,18-H; AB patterns; <sup>3</sup> $J_{AB} = 5$  Hz. <sup>c</sup> 3-H resonance not identified. <sup>d</sup> Overlapped with the benzoyl resonances.

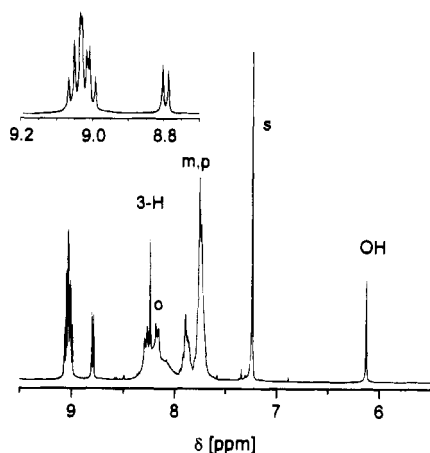
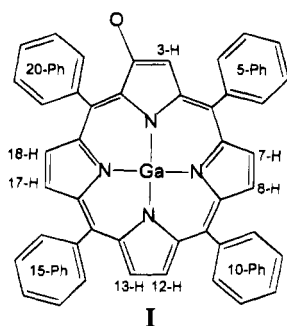


**Figure 4.** 300 MHz  $^1\text{H}$  NMR spectrum of (2-OH-TPP)Ga<sup>III</sup>Cl in chloroform-*d* at 293 K. The inset presents the expansion of the three AB patterns assigned to the pyrrole resonances. Resonance assignments follow those used in the text with OH indicating the  $\beta$ -hydroxyl proton.

trimer resonances is presented in structure I.



The proton resonances can be conveniently separated into four groups (Figure 3, traces B, B' and C, C'). The most characteristic features at 2.82, 2.18, and 1.82 ppm (243 K), correspond to the 3-H pyrrole protons (Figure 3, trace B). They are strongly upfield shifted, not scalar coupled, and their intensities correspond to one proton each. The remaining pyrrole protons produce nine AB patterns in the 7.35–9.00 ppm region (traces C and C', Figure 3). They are strongly overlapping with the complicated multiplets of the 5,10,15-phenyl resonances. These phenyl rings can contribute a maximum number of 45 resonances. The 20-phenyl resonances are unusually upfield shifted but three sets of the identical intensities are readily identified in the 5.2–7.1 ppm region (Figure 3, Trace B'). The spectrum in Figure 4 corresponds to a sample of [(2-O-TPP)Ga<sup>III</sup>]<sub>3</sub> to which gaseous HCl has been added. Its features are consistent with the cleavage to generate a monomeric (2-OH-TPP)Ga<sup>III</sup>Cl complex. A considerable simplification of the spectral pattern has been observed. The upfield 3-H pyrrole resonances, diagnostic of [(2-O-TPP)Ga<sup>III</sup>]<sub>3</sub>, have disappeared. Three new AB patterns are found in the 9.06–8.80

ppm region (Figure 4, Table 2). By comparison of  $^1\text{H}$  NMR spectra of (2-OH-TPP)Ga<sup>III</sup>Cl and (2-OH-TPP-*d*<sub>6</sub>)Ga<sup>III</sup>Cl (not shown), the resonance at 8.24 ppm has been assigned to the 3-H position at the  $\beta$ -substituted pyrrole. The selective deuteration of all but 3-H pyrrole positions has been accomplished for (2-OH-TPP-*d*<sub>6</sub>)Ga<sup>III</sup>Cl. The OH resonance has been observed at 6.12 ppm (293 K, CDCl<sub>3</sub>). When the chloroform-*d* saturated with deuterium oxide was added to the solution of (2-OH-TPP)Ga<sup>III</sup>Cl, the 2-OH peak disappeared. The 2-OH and 3-H resonances are scalar coupled over four bonds in the H–O–C–C–H fragment as established by a COSY experiment (293 K, CDCl<sub>3</sub>) although not resolved in the one-dimensional spectrum in Figure 4. The observation of the hydroxy resonance is consistent with the suggested mechanism of the cleavage process which requires the protonation in the 2-O position. The spectrum resembles one measured by Crossley et al. for (2-OH-TPP)Zn<sup>II</sup>.<sup>19</sup> The *meso* phenyl resonances are observed in the 7.7–7.9 (meta, para) and 8.0–8.3 ppm (ortho) regions as expected for typical gallium(III) tetraphenylporphyrins and are clearly distinct from those established for the trimeric precursor. The  $\beta$ -substitution markedly lowers the symmetry of the gallium(III) porphyrin from the effective  $C_{4v}$  symmetry of analogous (TPP)Ga<sup>III</sup>Cl. There are seven nonequivalent pyrrole positions. This is reflected in the  $^1\text{H}$  NMR spectra of (2-OH-TPP)Ga<sup>III</sup>Cl and (2-BzO-TPP)Ga<sup>III</sup>Cl (Table 2). In light of spectral characteristics of monomeric  $\beta$ -substituted gallium(III) tetraphenylporphyrin complexes, the  $^1\text{H}$  NMR spectrum of [(2-O-TPP)Ga<sup>III</sup>]<sub>3</sub> presents some suitable, analytically diagnostic features which can be only accounted for by the proximity of the three gallium(III) porphyrin units.

**Molecular Model of [(2-O-TPP)Ga<sup>III</sup>]<sub>3</sub>.** Molecular mechanics calculations have been used to visualize the suggested structure of the trimer and to evaluate the degree of the porphyrin distortion that is necessary to form this species. In the minimization procedure we have used the standard MM+ parameterization of the HyperChem program with the exception of the gallium coordination where constraints, reflecting the size of the gallium(III) ion, have been imposed. The characteristic features of gallium(III) tetraphenylporphyrins included the displacement of the ion from the plane of the four nitrogens (0.4 Å) and relatively long Ga–N bonds (2.05 Å). The structural parameters are in a range found for a variety of gallium(III) porphyrins by X-ray crystallography.<sup>24,25</sup>

All spectroscopic evidence indicated that the gallium(III) complex has a head-to-tail trimeric structure with the pyrrolic-alkoxide groups forming bridges from one macrocycle to the

- (24) (a) Coutsolelos, A.; Guillard, R.; Boukhris, A.; Lecomte, C. *J. Chem. Soc., Dalton Trans.* **1986**, 1779. (b) Boukhris, A.; Lecomte, A.; Coutsolelos, A.; Guillard, R. *J. Organomet. Chem.* **1986**, *303*, 151. (c) Coutsolelos, A.; Guillard, R.; Bayeul, D.; Lecomte, C. *Polyhedron* **1986**, *5*, 1157. (d) Serr, R.; B.; Headford, C. E. L.; Anderson, O. P.; Elliott, C. M.; Spartalian, K.; Fainzilberg, V. E.; Hatfield, W. E.; Rohrs, B. R.; Eaton, S. S.; Eaton, G. R. *Inorg. Chem.* **1992**, *31*, 5450.
- (25) Balch, A. L.; Hart, R. L.; Parkin, S. *Inorg. Chim. Acta* **1993**, *205*, 137.

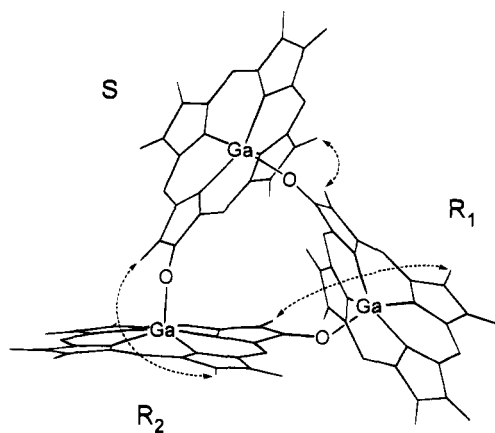


**Figure 5.** Drawing of the trimer  $[(2\text{-O-TPP})\text{Ga}^{\text{III}}]_3$  obtained from molecular mechanics calculation. Phenyl rings were omitted for clarity. The gallium(III) porphyrin subunits are labeled *S* and *R* as explained in the text. Arrows indicate the selected interporphyrin contacts, 3-H(*R*<sub>1</sub>)-17-H(*S*), 3-H(*S*)-17-H(*R*<sub>2</sub>), 3-H(*R*<sub>2</sub>)-7-H(*R*<sub>1</sub>), which are crucial in the interpretation of the NOE relays. These contacts are directly related to assigned cross-peaks (*c*, *g*, *j*) in the NOESY map, shown in Figure 6.

metal in the adjacent macrocycle  $\text{PGa-O-PGa-O-PGa-O}$ .

Such an oligomeric structure accounts for the molecular mass of the largest ion in the mass spectrometry. The  $^1\text{H}$  NMR spectrum clearly identifies three nonequivalent gallium(III) porphyrin units in the molecule as demonstrated by three upfield singlets and nine AB patterns of pyrrole protons (Figure 3). The unprecedented upfield chemical shift of 3-H resonances can be explained only by the direct coordination of the  $\beta$ -oxygen to another gallium(III) and the placement of the 3-H in the deshielding zone of the neighboring porphyrin (*vide infra*) as required by oligomerization. Finally, an alternative, linear, trimeric structure would require an OH resonance in the 5.0–6.5 ppm region that was not identified in the  $^1\text{H}$  NMR spectrum. In addition, the linear geometry of the trimer would generate only two 3-H pyrrole resonances, instead of the observed three.

Formally, gallium(III) 2-hydroxytetraphenylporphyrin (2-OH-TPP) $\text{Ga}^{\text{III}}\text{X}$  (X = any axial ligand) can be used as a building block in the oligomerization. In our previous work from this series, we presented the detailed consideration which led to the construction of the molecular model of the trimeric complex  $[(2\text{-O-TPP})\text{Fe}^{\text{III}}]_3$ .<sup>18</sup> The identical analysis is valid for the gallium(III) trimer. The five-coordinate (2-OH-TPP) $\text{Ga}^{\text{III}}\text{X}$  complexes exist as two optical antipodes (*R* and *S*).<sup>18</sup> During oligomerization the stereoisomeric mixture can be formed *RRR*, *SSS* ( $C_3$  symmetry) and *RRS*, *SSR* (pseudo- $C_3$  symmetry). However, the multiplicity of the porphyrin resonances of  $[(2\text{-O-TPP})\text{Ga}^{\text{III}}]_3$  is consistent solely with the symmetry of *RRS* and *SSR* enantiomers, which are indistinguishable by means of  $^1\text{H}$  NMR. The synthetic selection of the *RSS* and *SSR* enantiomers seems to be directed by structural factors intrinsic to the substrate molecules themselves. A schematic view of the *RRS* trimer skeleton as obtained by the molecular mechanics is presented in Figure 5. For the sake of clarity the phenyl rings have been omitted from the stick drawing although we have included them directly in the minimization procedure. The gallium(III) ions are located at corners of the equilateral triangle at a distance ca. 7 Å. The closest interporphyrin contacts are in the range observed in the structures of other metalloporphyrins.<sup>12c,26</sup>

**Assignment of the Proton Resonances.** Two-dimensional COSY experiments have been effective in connecting the

protons within *meso* phenyl and pyrrole rings. The upper left triangle of Figure 6 shows COSY data of  $[(2\text{-O-TPP})\text{Ga}^{\text{III}}]_3$  gathered in chloroform-*d* solution at 243 K. Cross-peaks reveal pairwise coupling among 18 pyrrole resonances. Characteristic sets of cross-peaks due to coupling between five protons of a ring have been established and located in the COSY map for 12 nonequivalent phenyls of the trimer. Representative examples are shown in Figure 6.

The complete peak assignments have been derived from the NOESY and ROESY experiments (Table 1). Here we only present the most fundamental steps of the discussion. The NOESY map for  $[(2\text{-O-TPP})\text{Ga}^{\text{III}}]_3$  collected at 243 K is illustrated in Figure 6 (lower right triangle and the right section). The ROESY experiment (the map not shown) gave identical qualitative results but allowed the straightforward differentiation of NOE and EXY cross-peaks.<sup>27–29</sup> We have started the analysis of the NOESY map from the unambiguous assignments in the most characteristic part (1.5–7.1 ppm) of the one-dimensional spectrum (Figure 3, Traces B and B'), where the 3-H and 20-phenyl resonances are located. Their shifts result from the considerable contribution of the neighboring porphyrin ring current effect. Considering in detail the spatial proximity of 3-H and 20-phenyls protons in the structural model, we have established that 20-phenyl(*R*<sub>1</sub>), 20-phenyl(*R*<sub>2</sub>), and 3-H(*S*) are located on the same side of the plane defined by three gallium(III) ions (Figure 5). The 3-H(*R*<sub>1</sub>), and 3-H(*R*<sub>2</sub>) protons and 20-phenyl(*S*) ring occupy the opposite side relative to this plane. On the basis of the relative distance comparison of ortho 20-Ph and 3-H protons, we could expect the NOE cross-peaks exclusively between ortho protons of 20-Ph(*R*<sub>1</sub>) and 20-Ph(*R*<sub>2</sub>) and a cross-peak between the ortho proton of 20-Ph(*R*<sub>2</sub>) and the 3-H(*S*). The unique cross-peak between the 3-H proton at 2.18 ppm and ortho at 5.21 ppm (*e*, Figure 6) allowed their recognition as the 3-H(*S*) and the ortho 20-Ph(*R*<sub>2</sub>), respectively. The ortho 20-Ph(*R*<sub>1</sub>) at 6.33 ppm is recognized by the cross-peak (*o*, Figure 6) to the ortho 20-Ph(*R*<sub>2</sub>). In each case the ortho resonances, which belong to the same phenyl ring, have been identified by the EXY cross-peaks in the NOESY and ROESY maps and the previously described COSY relays. The 20-Ph(*S*) phenyl could be identified by default. The strong interporphyrin interpyrrolic NOE cross-peaks from 3-H(*R*<sub>1</sub>) and 17-H(*S*) (*c*), 3-H(*S*) and 17-H(*R*<sub>2</sub>) (*g*), and 3-H(*R*<sub>2</sub>) and 7-H(*R*<sub>1</sub>) (*j*) are consistent with their geometrical proximity (Figures 5 and 6). At this stage we have unambiguously established the starting resonances to carry out further assignments for each unit of the trimer. The relays of observed and assigned NOE connectivities for each subunit separately are presented in Figure 7. The decisive sequence of the NOE effects to prove the cyclic trimeric structure is illustrated in Figure 6 (cross-peaks: *j*, *l*, *m*, *n*). We have established that this is the shortest full loop, which includes at once all units of the trimer. This path requires only the following through-space connectivities: 3-H(*R*<sub>2</sub>) – 5-Ph(*R*<sub>2</sub>, *o*<sub>2</sub>) – 20-Ph(*S*, *o*<sub>2</sub>) – 5-Ph(*R*<sub>1</sub>, *o*<sub>2</sub>) – 3-H(*R*<sub>2</sub>). Independently, we have presented the interporphyrin contacts for the pyrrole protons (Figure 5, dashed arrows) which have been reflected by the cross-peaks (*c*, *g*, *j*) in the NOE map (Figure 6). Combining the inter- and intraporphyrin connectivities, we could track down several independent looped NOE successions. We would like to point out that the cyclic trimeric structure is a prerequisite for such a spectral sequence.

(27) (a) Kessler, H.; Griesinger, C.; Kersebaum, R.; Wagner, E.; Ernst, R. *J. Am. Chem. Soc.* **1987**, *109*, 607. (b) Kessler, H.; Bats, J. W.; Griesinger, C.; Koll, S.; Will, M.; Wagner, K. *J. Am. Chem. Soc.* **1988**, *110*, 1033.

(28) (a) Bax, A.; Davis, D. G. *J. Magn. Reson.* **1985**, *63*, 207. (b) Bax, A.; Davis, D. G. *J. Magn. Reson.* **1985**, *64*, 533.

(29) Jeon, S.; Almarsson, Ö.; Karaman, R.; Blaskó, A.; Bruce, T. C. *Inorg. Chem.* **1993**, *32*, 2562.

(26) Scheidt, W. R.; Lee, Y. J. *Struct. Bonding* **1987**, *64*, 1.

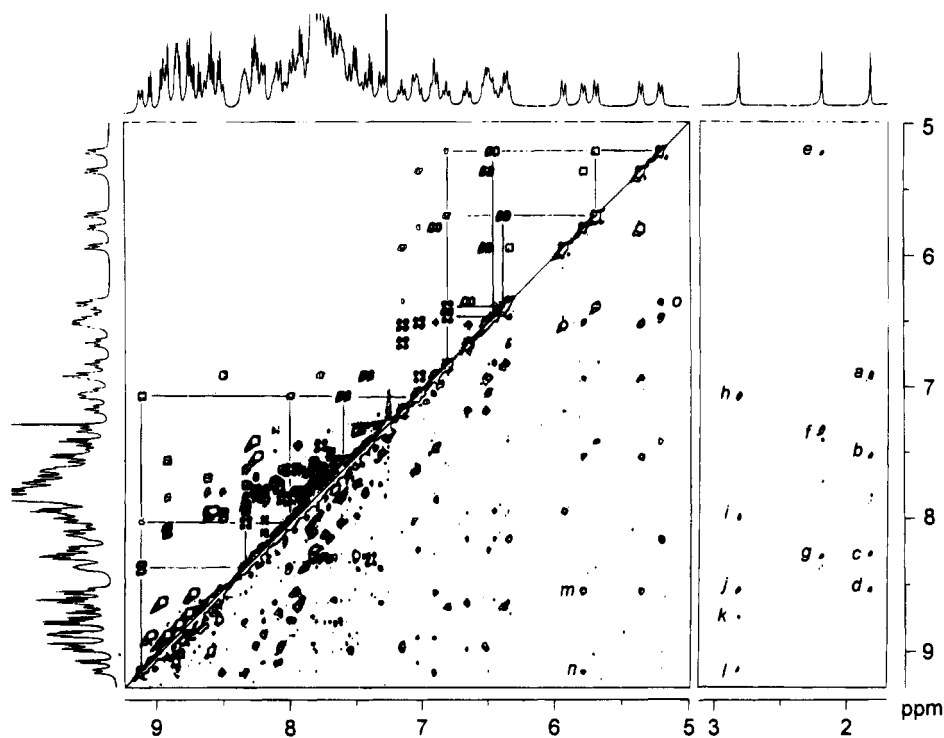


**Figure 6.** The 2D  $^1\text{H}$  NMR spectra of  $[(2\text{-O-TPP})\text{Ga}^{\text{III}}]_3$  in chloroform- $d$  at 243 K. The upper left triangle presents the COSY map, the bottom-right parts demonstrate the NOESY experiment. The representative examples of scalar connectivities (solid lines) for the selected phenyls: 20-Ph( $R_2$ ) and 5-Ph( $R_2$ ), are shown in the COSY map. The most characteristic cross-peaks, crucial to geometrical considerations, are labeled in the figure (the NOE part) as follows: *a*, 3-H( $R_1$ )–5-Ph( $R_1$ ,  $o_1$ ); *b*, 3-H( $R_1$ )–18-H(S); *c*, 3-H( $R_1$ )–17-H(S); *d*, 3-H( $R_1$ )–5-Ph( $R_1$ ,  $o_2$ ); *e*, 3-H(S)–20-Ph( $R_2$ ,  $o_1$ ); *f*, 3-H(S)–5-Ph(S,  $o_1$ ); *g*, 3-H(S)–17-H( $R_2$ ); *h*, 3-H( $R_2$ )–5-Ph( $R_2$ ,  $o_1$ ); *i*, 3-H( $R_2$ )–10-Ph( $R_1$ ,  $o_1$ ); *j*, 3-H( $R_2$ )–5-Ph( $R_1$ ,  $o_2$ ) and 7-H( $R_1$ ) (overlapped); *k*, 3-H( $R_2$ )–8-H( $R_1$ ); *l*, 3-H( $R_2$ )–5-Ph( $R_2$ ,  $o_2$ ); *m*, 20-Ph(S,  $o_2$ )–5-Ph( $R_1$ ,  $o_2$ ); *n*, 20-Ph(S,  $o_2$ )–5-Ph( $R_2$ ,  $o_2$ ); *o*, 20-Ph( $R_2$ ,  $o_1$ )–20-Ph( $R_1$ ,  $o_2$ ). The cross-peaks *c*, *g*, and *j* correspond to interporphyrin contacts indicated in Figure 5 (dashed arrows).

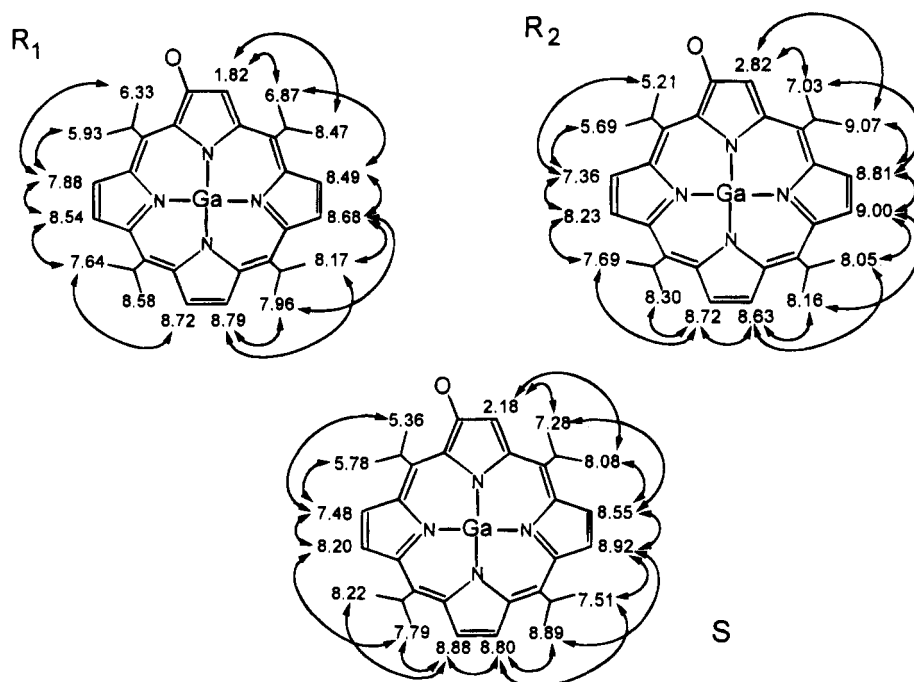


**Figure 7.** Established NOE connectivities (solid arrows) in subunits of the trimer  $[(2\text{-O-TPP})\text{Ga}^{\text{III}}]_3$ . The chemical shifts (in ppm) of pyrrole and ortho phenyl resonances are included. The phenyl rings are presented schematically.

**Temperature Dependence of the  $[(2\text{-O-TPP})\text{Ga}^{\text{III}}]_3$  Spectrum.** Two ortho and meta protons on each *meso* phenyl ring are unequivalent since the porphyrin plane bears different substituents on opposite sides and a rotation about the *meso* carbon-phenyl bond is sterically restricted. In particular the slow rotation is expected for 5-phenyl and 20-phenyl rings, which are located in the very crowded regions of the trimer structure. The analysis of the ROESY spectra allowed the identification of the characteristic EXY peaks between two ortho resonances

of each of the 20-phenyls. The EXY peaks were in the same phase as the corresponding diagonal ones contrary to the NOE cross-peaks with the opposite phases.<sup>28</sup> Since 20-phenyl rings are exposed to the different steric hindrance, we have anticipated noticeable differences in their rotation rates. The temperature dependence of the one-dimensional  $^1\text{H}$  NMR spectrum in the spectral region of 20-Ph ortho resonances is shown in Figure 8. The selective broadening of the 20-Ph(S) ortho signals has been determined to produce the deceptively simplified spectrum

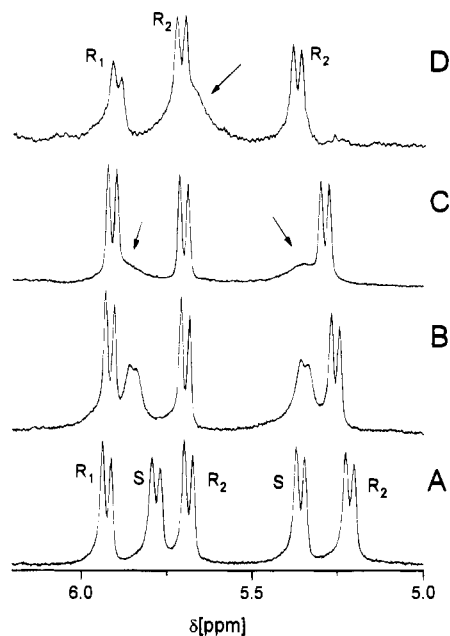


**Figure 8.** The ortho 20-phenyl region of the 300 MHz  $^1\text{H}$  NMR spectrum of  $[(2\text{-O-TPP})\text{Ga}^{\text{III}}]_3$  in chloroform-*d* solution as a function of the temperature: (A) 243 K; (B) 273 K; (C) 293 K; (D) 343 K (measured in the sealed NMR tube). Individual resonances were assigned to specific units of the trimer. One of the ortho( $R_1$ ) resonances (not shown) is overlapped with a meta multiplet. Arrows in Traces C and D indicate the broadened, due to the rotation, ortho 20-Ph ( $S$ ) resonances.

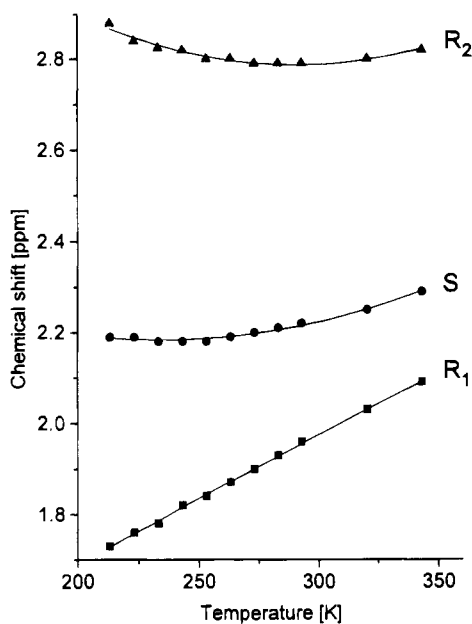


**Figure 9.** Temperature dependence of the chemical shifts of 3-H pyrrrole resonances of  $[(2\text{-O-TPP})\text{Ga}^{\text{III}}]_3$  in chloroform-*d*. The individual assignment to the specific unit of the trimer is shown in the figure.

at 293 K. The two crucial ortho peaks could be easily missed from the intensity count.

The unusual temperature dependencies of the chemical shifts for the pyrrrole resonances have been also observed and are shown in Figure 9. These temperature effects have been followed for 0.5 and 3 mM solutions and have been found concentration independent. This observation confirms their intramolecular mechanism.

In particular the chemical shift of the 3-H( $R_1$ ) proton smoothly increased from 1.73 ppm at 213 K to 2.09 ppm at 343 K. The changes at any other pyrrrole positions (3-H( $S$ ) and 3-H( $R_2$ )), although noticeable, are smaller. We have attributed these

**Table 3.** Selected Ring Current Shifts (ppm) for  $[(2\text{-O-TPP})\text{Ga}^{\text{III}}]_3$ <sup>a</sup>

proton	unit			
	$S$	$R_1$	$R_2$	
pyrrole	3-H	-6.78	-7.14	-6.14
	7-H	-0.50	-0.56	-0.24
	8-H	-0.13	-0.37	-0.05
	12-H	-0.25	-0.26	-0.42
	13-H	-0.17	-0.33	-0.33
	17-H	-0.78	-0.44	-0.75
<i>meso</i> -phenyl <sup>b</sup>	18-H	-1.31	-0.91	-1.43
	5-Ph $o_1$	-0.92	-1.33	-1.17
	$o_2$	-0.12	+0.27	+0.87
	20-Ph $o_1$	-2.59	-2.02	-2.74
$o_2$	-2.17	-1.62	-2.26	

<sup>a</sup> Calculated as the difference between proton chemical shifts of  $[(2\text{-O-TPP})\text{Ga}^{\text{III}}]_3$  and  $(2\text{-BzO-TPP})\text{Ga}^{\text{III}}\text{Cl}$  (243 K, chloroform-*d*). <sup>b</sup> Phenyl chemical shifts for  $(2\text{-BzO-TPP})\text{Ga}^{\text{III}}\text{Cl}$ : 5-Ph (ortho)  $\delta$  = 8.20 ppm, 20-Ph (ortho)  $\delta$  = 7.95 ppm.

differentiated changes to the dynamic process which takes place at the  $S$  subunit. The observed rotation of the 20-Ph( $S$ ) ring has to be accompanied by a change of the 3-H( $R_1$ ) proton position with respect to the porphyrin  $S$  plane. Actually, the concerted structural rearrangements of the  $S$ ,  $R_1$ , and  $R_2$  porphyrin macrocycles are required to allow the flip of the 20-phenyl ring in the very crowded region of the trimeric molecule. The ring current shift is very sensitive to the orientation of the 3-H( $R_1$ ) proton relative to the  $S$  porphyrin plane due to their vicinity. The estimated proton displacement by merely 0.1–0.2 Å is sufficient to cause the observed change of the chemical shift. The rigid structural model of  $[(2\text{-O-TPP})\text{Ga}^{\text{III}}]_3$  has been used to interpret the  $^1\text{H}$  NMR spectrum. However, in solution at the temperature range studied, one can expect several, slightly structurally different forms which may remain in the thermal equilibrium(a). This phenomenon is reflected through the discussed temperature dependency of the 3-H( $R_1$ ) chemical shift.

The ring current shifts, which resulted from the trimer formation have been evaluated by subtracting the chemical shift values for each proton in  $(2\text{-BzO-TPP})\text{Ga}^{\text{III}}\text{Cl}$  from those for the corresponding protons in  $[(2\text{-O-TPP})\text{Ga}^{\text{III}}]_3$ . The most characteristic values are gathered in Table 3. They reflect the thermally averaged values for all structures present in the system. To obtain independent evidence of the cyclic trimer formation for  $[(2\text{-O-TPP})\text{Ga}^{\text{III}}]_3$  the ring current shifts have been estimated using the double-loop model of Abraham et al.<sup>30</sup> Recently the geometry determination by way of ring current effect analysis was explored with success for cofacial covalently linked diporphyrins.<sup>31</sup>

In order to simplify the calculations of ring current effect, we have assumed a static trimeric structure in which all units of the trimer including mobile phenyl rings are fixed as in the earlier generated molecular model. This procedure gives the limits of ring current contributions for protons most exposed to the interporphyrin ring current: pyrroles 3-H, from -6.1 to -7.1; 18-H, from -0.7 to -3.3; phenyls, 20-Ph(ortho), from -0.5 to -3.7; 5-Ph(ortho), from -1.3 to 0.9 ppm. These values can be compared with the experimental data gathered in Table 3. In our opinion, considering the simplification imposed on dynamic properties of the structural model, the agreement in predicting the trends in the ring current contribution to the chemical shifts of the trimer is reasonable.

(30) (a) Abraham, R. J.; Fell, S. C. M.; Smith, K. M. *Org. Magn. Reson.* **1977**, *9*, 367. (b) Abraham, R. J.; Bedford, G. R.; MacNeillie, D.; Wright, B. *Org. Magn. Reson.* **1980**, *14*, 418.

(31) Uemori, Y.; Nakatsubo, A.; Imai, H.; Nakagawa, S.; Kyuno, E. *Inorg. Chem.* **1992**, *31*, 5164.

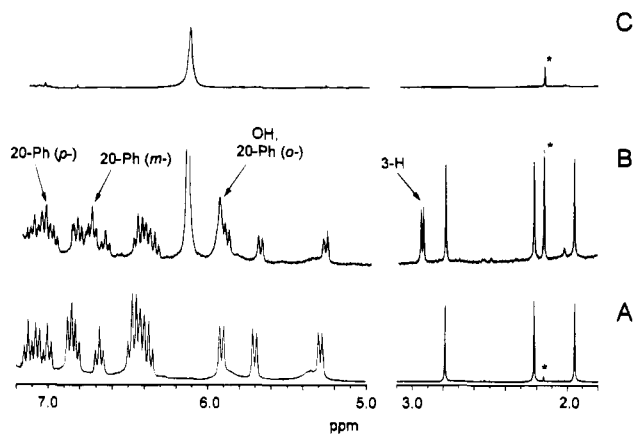


**Figure 10.**  $^1\text{H}$  NMR titration of  $[(2\text{-O-TPP})\text{Ga}^{\text{III}}]_3$  with TFA in chloroform- $d$  at 293 K: (A) 0 equiv; (B) 0.6 equiv; (C) 3 equiv of TFA added. The region corresponding to the resonances with the largest upfield ring current contribution is exclusively shown. Trace A presents the spectrum of  $[(2\text{-O-TPP})\text{Ga}^{\text{III}}]_3$ . The OH resonance of  $(2\text{-OH-TPP})\text{Ga}^{\text{III}}\text{TFA}$  is only seen in trace C. The ring current shifted resonances of the intermediate are labeled in trace B according to the convention used for the trimer.

**Cleavage of  $[(2\text{-O-TPP})\text{Ga}^{\text{III}}]_3$ .** Titration of  $[(2\text{-O-TPP})\text{Ga}^{\text{III}}]_3$  with trifluoroacetic acid (TFA) results in the stepwise cleavage of the trimer, described formally according to eq 3.

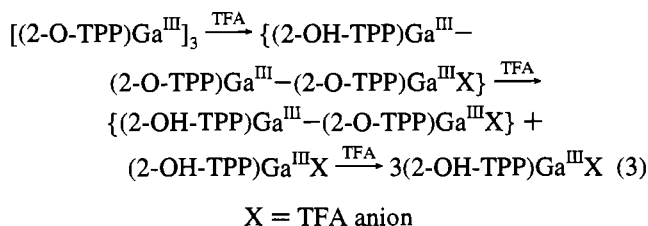
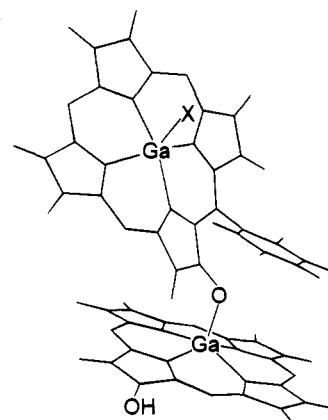


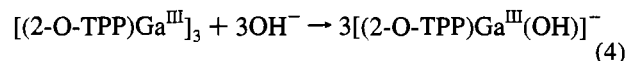
Figure 10 shows relevant  $^1\text{H}$  NMR spectra. Resonances of  $[(2\text{-O-TPP})\text{Ga}^{\text{III}}]_3$  and  $(2\text{-OH-TPP})\text{Ga}^{\text{III}}(\text{TFA})$  could be easily identified in the  $^1\text{H}$  NMR spectra collected during the titration. New resonances, existing in the presence of 0.1–0.8 equivs of acid, have been assigned to the linear expanded form. The spectrum in trace B shows a sample of  $[(2\text{-O-TPP})\text{Ga}^{\text{III}}]_3$  to which 0.6 equiv of trifluoroacetic acid has been added. The two 3-H resonances of equal intensities (2.96, 2.94 ppm), revealing the linear polymeric structure, are markedly shifted in the upfield direction as compared to those for the monomeric  $(2\text{-OH-TPP})\text{Ga}^{\text{III}}\text{TFA}$  although the effect is smaller than that seen for the trimer. By subtraction of the trimeric spectrum (trace A) from the spectrum reflecting the progress of titration (trace B), we have also identified a single set of broadened, upfield shifted, 20-phenyl resonances (ortho, 5.95; meta, 6.76; para, 7.03 ppm). The most characteristic 2-OH resonance, associated with a terminal unit of the polymer, has been found at 5.95 ppm. The other pyrrole and phenyl resonances are in the crowded part of spectrum (9–7 ppm) and are practically obscured by signals of the cyclic trimer and the monomer. The positions of the diagnostic 3-H pyrrole and phenyl resonances can be exclusively accounted for by the 2-O donor coordination to the adjacent gallium(III) porphyrin unit. Three structurally different linear trimers ( $RRS^*$ ,  $RSR^*$ ,  $SRR^*$  — the position of the OH group in the linear structure is marked by an asterisk) can be directly derived from the cyclic trimer, merely by a single cleavage of one from the three bridging 2-O–Ga(III) bonds. However, such a process should result in the presence of six, shifted in the upfield direction, pyrrole resonances in the  $^1\text{H}$  NMR spectrum, instead of the observed two, unless one from the three possible species is thermodynamically preferred. This spectral feature should be accompanied by the complex pattern



**Figure 11.** Drawing of the dimer  $(2\text{-OH-TPP})\text{Ga}^{\text{III}} - (2\text{-O-TPP})\text{Ga}^{\text{III}} - \text{TFA}$  obtained from molecular mechanics calculation (X = TFA). Only a 20-phenyl ring, exposed to the largest contacts with the adjacent macrocycle, is included in the dimetalloporphyrin skeleton.

of the 20-phenyl resonances in the 7.0–5.0 ppm region. The alternative explanation of the titration, favored by us, involves the random formation of expanded dimers. Two enantiomeric couples:  $RS^* - SR^*$  and  $RR^* - SS^*$  can be distinguished by  $^1\text{H}$  NMR. Their statistical occurrence implies the equal concentration of  $RS^*$  ( $SR^*$ ) and  $RR^*$  ( $SS^*$ ) digallium(III) species and only two 3-H pyrrole resonances with the identical intensities in the 1.5–3.5 ppm region. Only one from two 3-H protons in the dimer is exposed to the very strong ring current effect imposed by the coordination of 2-O oxygen to gallium(III), although the 3-H shifts should be slightly different for each diastereoisomer. Molecular mechanics calculations have been used to visualize the dimeric expanded structure (Figure 11). The linear expansion of the molecule releases crowding encountered in the trimer. This is reflected by smaller ring current shift of 3-H and 20-Ph phenyl resonances when compared to the trimer spectral parameters. In the analogous acidic cleavage of iron(III) trimer  $[(2\text{-O-TPP})\text{Fe}^{\text{III}}]_3$  we have also established solely the dimeric expanded intermediate.<sup>18</sup>

Addition of sodium hydroxide in methanol- $d_4$  to a solution of  $[(2\text{-O-TPP})\text{Ga}^{\text{III}}]_3$  in chloroform- $d$  has been followed by  $^1\text{H}$  NMR. It resulted in the trimer conversion to the green five-coordinate complex:



Three AB patterns are assigned to 7, 8; 12, 13; and 17, 18 pyrrole couples (Table 2). The 3-H pyrrole resonance has not been identified. Addition of water to chloroform solution of  $[(2\text{-O-TPP})\text{Ga}^{\text{III}}(\text{OH})]^-$  resulted in the reversion to the trimer.

**Keto–Enol Tautomerism in  $(2\text{-OH-TPP})\text{Ga}^{\text{III}}\text{Cl}$ .** During the synthesis of the pyrrole deuterated  $[(2\text{-O-TPP})\text{Ga}^{\text{III}}]_3$ , we have observed the increased lability of the 3-H proton. The usual procedure of the trimer synthesis has been modified by the replacement of  $(2\text{-BzO-TPP})\text{Ga}^{\text{III}}\text{Cl}$  with  $(2\text{-BzO-TPP-}d_7)\text{Ga}^{\text{III}}\text{Cl}$  (80% deuteration measured by  $^1\text{H}$  NMR). The intensity of the three upfield shifted singlet pyrrole resonances has been preserved in the  $^1\text{H}$  NMR spectrum of  $[(2\text{-O-TPP-}d_6)\text{Ga}^{\text{III}}]_3$  (not shown) contrary to the reduced intensity of the remaining pyrrole signals. To account for the process of the deuterium–proton exchange we have considered the keto–enol tautomerism established by Crossley et al. for zinc(II) and copper(II) complexes of 2-hydroxytetraphenylporphyrin<sup>19</sup> and observed also for  $[(2\text{-O-TPP})\text{Fe}^{\text{III}}]_3$  and related monomeric complexes.<sup>18</sup> The  $(2\text{-OH-TPP})\text{Ga}^{\text{III}}\text{Cl}$  complex contains almost entirely hydroxyporphyrin tautomer because its  $^1\text{H}$  NMR spectrum demonstrates the hydroxyl resonance. The increased



contribution of the keto tautomer for [(2-O-TPP)Ga<sup>III</sup>(OH)]<sup>-</sup> in comparison to (2-OH-TPP)Ga<sup>III</sup>Cl is shown by the upfield change of all pyrrole shifts (Table 2).

## Conclusions

The oligomerization process of monomeric gallium(III) 2-hydroxy-5,10,15,20-tetraphenylporphyrin results in formation of a novel cyclic trimeric complex. The cyclic trimeric structure has been confirmed through the detailed one- and two-dimensional <sup>1</sup>H NMR investigations. The ring current shift patterns present several analytically useful probes for detecting the analogous trimeric species for diamagnetic systems by <sup>1</sup>H NMR spectroscopy. The spectroscopic evidence indicates that the gallium(III) complex has a head-to-tail trimeric structure with the pyrrolic-alkoxide groups forming bridges from one macrocycle to the metal in the adjacent macrocycle of PGa-O-PGa-O-PGa-O. The structurally sophisticated building elements [R,S-(2-O-TPP)Ga<sup>III</sup>] are found to self-assemble with unexpected stereoselectivity.

## Experimental Section

All solvents were purified by standard procedures. Tetraphenylporphyrin (TPPH<sub>2</sub>), TPPH<sub>2</sub>-*d*<sub>8</sub> deuterated at β-pyrrole positions, and TPPH<sub>2</sub>-*d*<sub>20</sub> deuterated at β-pyrrole positions, and TPPH<sub>2</sub>-*d*<sub>20</sub> deuterated at *meso* phenyl rings, were prepared using reported methods.<sup>32,33</sup> Benzaldehyde-*d*<sub>5</sub>, used in the synthesis of TPPH<sub>2</sub>-*d*<sub>20</sub>, was obtained by oxidation of toluene-*d*<sub>8</sub> with Ce(NH<sub>4</sub>)<sub>2</sub>(NO<sub>3</sub>)<sub>6</sub>.<sup>34</sup> 2-(Benzoyloxy)tetraphenylporphyrin, 2-BzO-TPPH<sub>2</sub>, was prepared using standard procedures starting from TPPH<sub>2</sub>.<sup>18,20</sup> The respective deuterated derivatives were obtained from the deuterated precursors. Chloroform-*d* (CDCl<sub>3</sub>, Glaser AG) was dried before use by passing it through basic alumina.

**(2-BzO-TPP)Ga<sup>III</sup>Cl.** A solution of 200 mg (1.2 mmol) of gallium(III) chloride (Serva) in 50 mL of ethanol was added to a solution of 100 mg (0.135 mmol) of (2-benzoyloxy)tetraphenylporphyrin in 150 mL of chloroform. Sodium carbonate was added to adjust the acidity of the reaction mixture. The purple solution was heated under reflux for 0.5 h. It was cooled, washed three times with water, and dried over anhydrous magnesium sulfate. After filtration, solvent was removed on the rotary evaporator. The solid residue was dissolved in chloroform and subjected to column chromatography on a silica gel column. Elution with chloroform gave the fraction containing 2-BzO-TPPH<sub>2</sub>. Further elution with chloroform/methanol (97:3 v/v) produced a pink-red fraction containing (2-BzO-TPP)Ga<sup>III</sup>Cl that was recovered from the solution as violet powder (60–70%). The product was identified by means of electronic spectroscopy and <sup>1</sup>H NMR.

UV-vis (CH<sub>2</sub>Cl<sub>2</sub>), λ<sub>max</sub>/nm (log ε): 422 (Soret, 5.42), 513 (3.44), 551 (4.02), 588 (3.41).

**[(2-O-TPP)Ga<sup>III</sup>]<sub>3</sub>** (2-BzO-TPP)Ga<sup>III</sup>Cl (60 mg, 0.072 mmol) was dissolved in 100 mL of ethanol and heated under reflux. Three to five pellets of sodium hydroxide were added to this solution. The color changed from pink-red to green. After 15 min, heating was discontinued. The reaction mixture was diluted with dichloromethane and washed several times with aqueous NaOH and water. The organic layer was separated, dried with anhydrous magnesium sulfate. The solid material was filtered off, and the filtrate was dried on the rotary evaporator. The dichloromethane solution of the solid residue was subjected to chromatography on a basic alumina column. Elution with dichloromethane gave the green-red fraction that was recovered as the solid after removal of the solvent under vacuum. Recrystallization of this solid from the dichloromethane/*n*-hexane (1/1 v/v) produced 35 mg of [(2-O-TPP)Ga<sup>III</sup>]<sub>3</sub> which precipitated as the violet powder, yield 70%.

UV-vis (CH<sub>2</sub>Cl<sub>2</sub>), λ<sub>max</sub>/nm (log ε, per gallium porphyrin unit): 405 (Soret, 5.16), 547 (4.09), 564 (4.05), 612 (3.85). MS (LSIMS): Calculated for C<sub>132</sub>H<sub>81</sub>N<sub>12</sub>O<sub>3</sub>Ga<sub>3</sub> (*m* + 1)/*z* = 2092; Found: (*m* + 1)/*z* = 2092. Anal. Calcd for C<sub>132</sub>H<sub>81</sub>N<sub>12</sub>O<sub>3</sub>Ga<sub>3</sub>: C, 75.77; N, 3.90; O, 8.03; Found: C, 75.80; N, 3.86; O, 8.06.

[(2-O-TPP-*d*<sub>6</sub>)Ga<sup>III</sup>]<sub>3</sub> and [(2-O-TPP-*d*<sub>20</sub>)Ga<sup>III</sup>]<sub>3</sub> were synthesized by following the procedure elaborated for [(2-O-TPP)Ga<sup>III</sup>]<sub>3</sub>.

**(2-OH-TPP)Ga<sup>III</sup>Cl.** Hydrogen chloride in dichloromethane was added to the solution of [(2-O-TPP)Ga<sup>III</sup>]<sub>3</sub> in dichloromethane (the color changed from green-red to pink-red). The solution was evaporated to dryness and the solid residue recrystallized from dichloromethane/*n*-hexane (1/1 v/v).

UV-vis (CH<sub>2</sub>Cl<sub>2</sub>), λ<sub>max</sub>/nm (log ε): 420 (Soret, 5.48), 510 (sh), 550 (4.33), 592 (3.87).

The bromo derivative was prepared by stirring the dichloromethane solution of [(2-O-TPP)Ga<sup>III</sup>]<sub>3</sub> with 1 M aqueous HBr. The organic layer was separated, dried, and evaporated to dryness, yielding (2-OH-TPP)Ga<sup>III</sup>Br as a violet powder.

**Cleavage Procedures.** Solutions of known concentration (2–3 mM in chloroform-*d* for <sup>1</sup>H NMR, 0.01–0.1 mM in dichloromethane for UV-vis spectroscopy) of the trimeric complex [(2-O-TPP)Ga<sup>III</sup>]<sub>3</sub> were prepared. The respective solution of the cleaving reagent (trifluoroacetic acid in chloroform-*d*, NaOH in methanol-*d*<sub>4</sub>) was titrated by a syringe, and the progress of the reaction was monitored by <sup>1</sup>H NMR or UV-vis spectroscopy.

**Molecular Mechanics Calculation.** Molecular mechanics calculations using HyperChem software (Autodesk) were carried out and displayed on the IBM 486 computer. The standard MM+ force field with the constraints set on the Ga–N coordination bonds to achieve the typical gallium(III) porphyrin geometry was used as described in the text.

**NMR Experiments.** <sup>1</sup>H NMR spectra were recorded on a Bruker AMX spectrometer operating in the quadrature mode at 300 MHz. The residual <sup>1</sup>H NMR resonances of the deuterated solvents were used as a secondary reference. A COSY spectrum of [(2-O-TPP)Ga<sup>III</sup>]<sub>3</sub> was obtained after collecting the standard 1D reference spectrum. The 2D COSY spectrum was acquired with 2048 points in *t*<sub>2</sub> over desired bandwidth (to include all desired peaks) and 512 *t*<sub>1</sub> blocks with 44 scans per block. Prior to Fourier transformation, the 2D-matrix was multiplied in each dimension with a 10° shifted sine-bell squared window function and zero filled to obtain a 1024 × 1024 word square matrix. The NOESY (NOESYTP) spectrum of [(2-O-TPP)Ga<sup>III</sup>]<sub>3</sub> was collected by use of 2048 points in *t*<sub>2</sub> and 512 in *t*<sub>1</sub> and 30 scans per *t*<sub>1</sub> block. The mixing time τ<sub>m</sub> = 900 ms was used. Prior to Fourier transformation the 2D matrix was multiplied in each dimension with a 8° shifted sine-bell squared window function and zero-filled to obtain a 1024 × 1024 word square matrix. ROESY spectra have been collected using the pulse sequence: 90°-*t*<sub>1</sub>-τ<sub>m</sub>-acquisition.<sup>28</sup> The mixing time τ<sub>m</sub> = 200 ms and a locking field strength of 1800 Hz were used. Spectra were collected into 2K blocks for 512 *t*<sub>1</sub> increments with a relaxation delay of 2 s. A data matrix was zero filled to 1K × 1K. Data were processed with a squared 7°-phase-shifted sine-bell in both dimensions and Fourier transformed in the phase sensitive manner. The ROESY spectrum was phase corrected and base line straightened.

**Instrumentation.** Absorption spectra were recorded on a Specord M-42 spectrometer and on a diode array Beckman 7500 spectrophotometer. Fluorescence spectra were measured on a SPF-500 (SLM AMINCO) instrument. Mass spectra were recorded on an AD-604 spectrometer using the liquid matrix secondary ion mass spectrometry technique and a primary beam of 8 keV Cs<sup>+</sup> ions.

**Acknowledgment.** The financial support of the State Committee for Scientific Research KBN (Grant 2 2651 92 03) is kindly acknowledged. Authors are grateful to Jarosław Tomczak for his assistance in calculations of ring current shifts.

IC940789C

(32) Lindsey, J. S.; Schreiman, I. C.; Hsu, H. C.; Kearney, P. C.; Marguerettaz, A. M. *J. Org. Chem.* **1987**, *52*, 827.

(33) Boersma, A. D.; Goff, H. M. *Inorg. Chem.* **1982**, *21*, 581.

(34) Syper, L. *Tetrahedron Lett.* **1966**, *37*, 4493.